Version of Record at: https://doi.org/10.1002/agj2.21554

Received: 6 July 2023 | Accepted: 3 February 2024

DOI: 10.1002/agj2.21554

Agronomy Journal

ORIGINAL ARTICLE

Crop Economics, Production, and Management

# Assessing relationships of cover crop biomass and nitrogen content to multispectral imagery

**Jarrod O. Miller** | **Amy L. Shober** | **Jamie Taraila**

Department of Plant and Soil Sciences, University of Delaware, Newark, Delaware, USA

**Correspondence**
Jarrod O. Miller, Department of Plant and Soil Sciences, University of Delaware, Newark, DE, USA.
Email: jarrod@udel.edu

Assigned to Associate Editor Yuxin Miao.

**Funding information**
Natural Resources Conservation Service, Grant/Award Number: #NR1821J2XXXXC003

**Abstract**

Cover crops provide valuable roles in sustainable agriculture, provided they produce enough biomass. To accurately measure their services to field management, spatial estimates would be useful to producers. This study used multispectral drone imagery to produce maps of normalized difference vegetation index (NDVI), normalized difference red edge index (NDRE), and a digital surface model (DSM) of cover crop plots on sandy, Mid-Atlantic soils. Cover crops included cereal rye (*Secale cereale*), mixtures of rye and crimson clover (*Trifolium incarnatum*), and mixtures of rye and hairy vetch (*Vicia villosa*). Their biomass was sampled in the spring of 2019, 2020, and 2021, dried, weighed, and analyzed for total nitrogen (N) content. Measurements of NDVI became saturated (i.e., reached a linear plateau) at 3.86 Mg biomass ha$^{-1}$, NDRE at 5.72 Mg biomass ha$^{-1}$, and the DSM at 5.11 Mg biomass ha$^{-1}$. The measured N content became saturated at 80.9, 139.1, and 75 kg N ha$^{-1}$ for NDVI, NDRE, and the DSM, respectively. Based on log transformations, NDVI was a stronger predictor of biomass and N, but not C:N. The NDRE was important for biomass, N, and C:N, while the DSM interactions with cover crop species helped predict both the N content and C:N of cover crop tissues. Accumulated growing degree days was important as an individual variable for biomass and N and as an interaction with cover crop species.

## 1 | INTRODUCTION

Measuring cover crop biomass is crucial for assessing their capacity to provide ecosystem services in sustainable agriculture (Finney et al., 2016; Garba et al., 2022; Otte et al., 2019; Teasdale et al., 2012). For instance, to achieve maximum weed suppression, cover crop biomass should ideally reach 4.6 Mg ha$^{-1}$, while for optimal $NO_3$-N retention, it should be around 6.9 Mg ha$^{-1}$ (Finney et al., 2016). Estimates of field scale cover crop biomass would help cash crop producers balance ecosystem services with potential yield losses due to cover crops, which will vary due to management and landscape variables (Deines et al., 2023; Yuan et al., 2019). Of particular interest is the estimations of nitrogen (N) within cover crop biomass, which could be considered a measure of $NO_3^-$ removal (or legume contributions to cash crops (White et al., 2019; Yuan et al., 2019).

Precision mapping of biomass offers an efficient solution to create field scale cover crop maps. Various sensing methods, including handheld, drone-mounted, and satellite-based sensors, have been employed for cover crop measurements

**Abbreviations:** DSM, digital surface model; GDD, growing degree days; NDRE, normalized difference red edge index; NDVI, normalized difference vegetation index.

Version of Record at: https://doi.org/10.1002/agj2.21554


(Corti et al., 2023; Prabhakara et al., 2015; White et al., 2019). These sensors have been used to measure biomass through vegetation indices (VIs), such as the normalized difference vegetation index (NDVI), triangular vegetation index (TVI), or Green NDVI (Prabhakara et al., 2015; Yuan et al., 2019). While VIs have performed well at estimating cover crop biomass, they can reach saturation points, as seen with NDVI when biomass exceeds 1.5 Mg $ha^{-1}$ (Prabhakara et al., 2015).

Besides VI, the incorporation of satellite-derived radar (SAR) alongside red-edge NDVI in regression models improved biomass estimations, although they still plateaued at 1.9 Mg $ha^{-1}$ (Jennewein et al., 2022). SAR is utilized in remote sensing to estimate plant heights, while drone-derived point clouds have enhanced stepwise linear regression models for crop height estimation (Corti et al., 2023; Kümmerer et al., 2023; Sangjan et al., 2022). Handheld cameras have also leveraged point clouds to improve biomass estimates for grass cover crops, with improvements of up to 8.0 Mg $ha^{-1}$ reported (Dobbs et al., 2023). Drone imagery has been used to estimate cover crop biomass and canopy height, but so far, it has been predominantly based on visual (red, green, blue, commonly known as "RGB") imagery rather than modeling with VIs (Kümmerer et al., 2023).

Besides biomass, the application of VIs to map N contents has also been successfully accomplished using handheld sensors (White et al., 2019), satellites (Xia et al., 2021), and drones (Yuan et al., 2019). Similar to biomass estimation, indices like NDVI and green-based NDVI have shown promise in estimating N uptake (Yuan et al., 2019), although their performance may vary (Xia et al., 2021). Another promising index for measuring cover crop N contents is the normalized difference red edge index (NDRE). While NDRE is commonly used to assess N status in corn (Bean et al., 2018), its application in measuring cover crop N contents has been relatively limited. Nevertheless, NDRE has demonstrated effectiveness in detecting chlorophyll content in plant leaves (Boiarskii & Hasewaga, 2019) and successfully distinguishing between cover crop species (Czarnecki et al., 2023). It holds potential as a reliable estimator of overall N contents.

While NDVI can effectively estimate biomass when it is below 1.5 Mg $ha^{-1}$, this estimation can be complicated due to variations in growth and management strategies. Farmers employ various cover crop management strategies, with termination timing being one of them. The accumulation of growing degree days (GDD), whether from earlier fall planting or later termination, should result in greater biomass (Balkcom et al., 2015; Baraibar et al., 2020; Butler et al., 2002; Otte et al., 2019; Pantoja et al., 2016; Reed et al., 2019; Thieme et al., 2023).

For instance, early boot cereal rye (Secale cereale) biomass can be as low as 1.4 Mg $ha^{-1}$ but can reach 7.1 Mg $ha^{-1}$ at later growth stages (Duiker & Curran, 2005), and has even been reported as high as 11 Mg $ha^{-1}$ in some Maryland fields (Thieme et al., 2023). However, GDD, an important predictor of plant growth, will not explain biomass production in all instances (Jennewein et al., 2022).

Other factors contributing to biomass development include fall soil $NO_3^-$ availability (Baraibar et al., 2020; Pantoja et al., 2016; Prabhakara et al., 2015) and seasonal rainfall (Brennan & Boyd, 2012; Otte et al., 2019). Biomass development can also be influenced by species selection (e.g., grass vs. legume) or the composition of species mixes (Brennan & Boyd, 2012; Finney et al., 2016; Pantoja et al., 2016; Poffenbarger et al., 2015).

Remote sensing of cover crop characteristics has varied by species, where red clover (*Trifolium incarnatum*) had stronger relationships than rye (Xia et al., 2021). Additionally, relationships with N content can vary by region, with stronger correlations in northeastern compared to mid-west cover crop fields (Xia et al., 2021).

Furthermore, algorithms for measuring cover crop characteristics can vary by cover crop species for both fall and spring measurements (White et al., 2019; Xia et al., 2021). Even when species are not considered, additional challenges in using remote sensing can arise during the growing season. Calibration equations using NDVI may require separate algorithms in the winter and spring (Theime et al., 2023). Additionally, winter freeze events may cause the senescence of leaf tissue, which is not measured by NDVI, even if the leafy biomass remains. (Holzhauser et al., 2022; Prabhakara et al., 2015).

The use of drones, or uncrewed aerial vehicles (UAV), is being explored across crop production (Gao & Zhang, 2021; Meresma et al., 2020; Poley & McDermid, 2020) and is expanding into cover crop measurements (Corti et al., 2023; Yuan et al., 2019). Drones provide higher resolution than satellites and can be flown on demand, depending on local weather. Of the previous studies performed with drones, there was limited use of either NDRE or crop heights as estimated by point clouds. The objectives of this study were to (1) explore the use of drone-derived VIs (NDVI and NDRE) to estimate cover crop biomass, (2) estimate N content when rye

**Core Ideas**

- Drone-derived NDVI, along with GDD, were strong predictors of biomass.
- As an individual variable, normalized difference red edge index was useful for predicting biomass, total N, and C:N.
- The digital surface model could predict N and C:N as an interaction with cover crop types.

Version of Record at: https://doi.org/10.1002/agj2.21554


**TABLE 1** Dates of cover crop termination and biomass/drone data collection prior to planting corn or soybean in small plots at the University of Delaware Carvel Research and Education Center in Georgetown, DE.

| | | Early termination dates (GDD) | | Late termination dates (GDD) | |
|---|---|---|---|---|---|
| **Trial year** | **Planting date** | **Corn** | **Soybean** | **Corn** | **Soybean** |
| 2019 | October 10 | April 17 (1576) | April 29 (1778) | April 29 (1778) | May 14 (2038) |
| 2020 | September 30 | March 30 (1552) | May 13 (2064) | April 17 (1747) | May 26 (2279) |
| 2021 | October 07 | April 14 (1521) | April 26 (1653) | April 26 (1653) | May 10 (1898) |

*Note*: Growing degree days (GDD) are shown in parenthesis.

was mixed with legumes, and (3) examine if crop height as estimated by a digital surface model (DSM) could improve estimates of both biomass and N contents.

## 2 | MATERIALS AND METHODS

### 2.1 | Study location and design

Two cover crop studies (for corn and soybean cash crops) were planted at the University of Delaware Carvel Research and Education Center in Georgetown, DE. The predominant soil series in the study area was Pepperbox loamy sand (loamy, mixed, semiactive, mesic Aquic Arenic Paleudult). For each cash crop, three fall planted cover crop treatments, cereal rye (*Secale cereale*), rye and crimson clover (*Trifolium incarnatum*), and rye and hairy vetch (*Vicia villosa*), and a no-cover control were planted in a randomized complete block design with four replications. Plots (3 m × 12 m) were planted into corn (*Zea mays* L.) or soybeans (*Glycine max* L.) in the subsequent spring following termination of the cover crop (Table 1). We included two cover crop termination timings at 2 weeks prior to planting corn or soybeans (early) or at planting (i.e., planting green); cover crops were terminated with glyphosate (Table 1). The soybean and corn studies were treated separately but were planted beside each other in the same field. GDD were calculated using temperature data from the Delaware Environmental Observatory System (DEOS: http://www.deos.udel.edu/), a mesonet for the state of Delaware. Using the Georgetown, DE, weather station data, we calculated GDD from the cover crop planting date to termination, using 0˚C as the base temperature.

$$\mathrm{GDD} = \frac{\text{Minimum temperature} + \text{maximum temperature}}{2} - 0^\circ\mathrm{C}$$

### 2.2 | Drone image acquisition and processing

Cover crop plots were mapped by drone imagery during each season, acquired on sunny or consistently overcast days with the sun greater than 30˚ in the sky. This imagery was acquired with a Parrot Disco Pro Ag fixed and a Parrot Sequoia multispectral camera during the 2019 spring season. For the spring of 2020 and 2021, we used a DJI Matrice 210 V2 quadcopter combined with a Micasense Altum multispectral camera. A 75% side and front overlap was used for flights 76 m above ground level, providing a 6.9 and 3.3 cm pixel$^{-1}$ resolution for the Seqouia and Altum cameras, respectively. To correct for spatial location, ground control points were marked using an Emlid Reach RS2+ RTK GPS receiver using the EGM96 Geoid for elevation. To correct for lighting conditions, a Micasense reflectance panel was photographed prior to each flight for incorporation into photogrammetric software.

Pix4DMapper was used to stich imagery into orthomosaics using the default agricultural settings for processing with the addition of calculating NDVI, NDRE, and the DSM as outputs. Within Pix4DMapper, the VIs are calculated with near-infrared (NIR) and red-edge (RE) bands as follows:

$$\mathrm{NDVI} = \frac{\mathrm{NIR} - \mathrm{Red}}{\mathrm{NIR} + \mathrm{Red}}$$

$$\mathrm{NDRE} = \frac{\mathrm{RE} - \mathrm{Red}}{\mathrm{RE} + \mathrm{Red}}$$

The agricultural settings were adjusted to use the triangulation method for crop surfaces to create the raster DSM GeoTiff. The NDVI, NDRE, and the DSM*.TIF were imported into geodatabase files in ArcGIS Pro (ESRI). A polygon-shaped file for each year was created to extract average NDVI, NDRE, and the DSM values for each cover crop plot. A digital elevation model (DEM, meters) derived from LiDAR data was used to subtract baseline elevation and estimate plant height, still referred to as the DSM (meters) in the manuscript. Average index and the DSM values were extracted from each geodatabase file using zonal statistics as a table with a plot polygon as the feature layer.

At cover crop termination (after imagery collection), two 0.5 m by 0.5 m templates were placed in each cover crop plot, and all aboveground biomass was removed as close to the soil surface as possible. Biomass subsamples were composited by plot, and the sample was oven dried, weighed, and analyzed for carbon (C) and N content by combustion at the University of Delaware Soil Testing Lab. Total cover crop biomass (Mg ha$^{-1}$) and N content (kg ha$^{-1}$) were estimated by dividing harvested biomass and N content by the quadrat sample.

Version of Record at: https://doi.org/10.1002/agj2.21554


## 2.3 | Data analyses

In this study, we conducted a series of analyses to investigate the relationships between VIs, harvest cover crop biomass, and nitrogen (N) content from each plot. First, we performed correlation analyses using the Proc Corr procedure in SAS (Statistical Analyses System) software (version 9.4, SAS Institute) to assess the associations between the VIs and the variables of interest, including cover crop biomass and total N content. Subsequently, we used the Proc NLin procedure to fit various regression models, with the specific aim of examining the occurrence of plateaus, indicating VI saturation of harvested biomass. The relationship was examined between harvested biomass, nitrogen content, and NDVI, NDRE, and the DSM. We considered several model forms, including linear, quadratic, quadratic plateau, and linear plateau models. The selection of the most appropriate model was based on the Akaike information criterion (AIC), with models having the lowest AIC values being chosen as the best-fitting models. We assessed the normality of the cover crop biomass data using the Proc Univariate procedure. The data were initially found to exhibit right-skewness and depart from normality assumptions based on tests, including the Shapiro-Wilk test. To address the skewness, we explored two common data transformation methods: log transformation and square root transformation. After applying both transformations separately, we compared their effects on normality using the univariate procedure. The log transformation was identified as the more effective choice in terms of bringing the data distribution closer to normality, as indicated by higher test statistics and *p*-values. The log-transformed data were used in subsequent analyses.

Using SAS software, we conducted a comprehensive modeling analysis that included single variables such as NDVI, NDRE, the DSM, GDD, and cover crop species (rye, rye–clover, and rye–vetch). Additionally, we explored interactions between cover crop species and the indices, as well as interactions involving GDD and the indices.

To identify the most appropriate model for predicted biomass or nitrogen contents, we used Proc GLMselect, incorporating cover crop species in the class statement. We used stepwise, forward, and backward selection to model the data. These approaches allowed us to systematically evaluate different combinations of predictor variables and interactions. The selection of the best-fitting model was guided by the AIC and cross-validation. The AIC was used in the select statement to quantify goodness of fit, where models with lower AIC were selected. Cross-validation was employed to assess the predictive performance of each model. It involved partitioning the data into training and validation sets, allowing us to estimate how well each model generalized to unseen data. We stopped the selection process when cross-validation indicated a suitable model.

Subsequently, we generated predicted datasets for each selected model. These datasets included predicted values of biomass or nitrogen content based on the chosen models and their associated parameter estimates. To account for the effects of different cover crop types on the relationship between VIs and cover crop characteristics, we incorporated dummy variables for cover crop categories. To visually assess the goodness-of-fit for each selected model, we created scatter plots comparing predicted values to observed values using data exported to CSV files.

# 3 | RESULTS AND DISCUSSION

## 3.1 | Plateau relationships of cover crop biomass with NDVI, NDRE, and the DSM

Throughout the 3-year duration of the study, the GDD at harvest ranged from 1521 to 2279, as summarized in Table 1. Cover crop biomass over that period ranged from an overall average of 4.31, 6.10, and 4.93 Mg ha$^{-1}$ in the rye, rye–clover, and rye–vetch plots, respectively (Table 2). These values are consistent with typical cover crop biomass measurements reported within the Mid-Atlantic region of the United States. Previous studies (Duiker & Curran, 2005; Theime et al., 2022) have reported cover crop biomass values ranging from 7 to 11 Mg ha$^{-1}$. However, the average values observed in our study closely align with the averages reported in other studies (Finney et al., 2016). The control plots represent winter weed biomass and ranged from a low of 1.09 to values close to minimum rye (4.09 Mg ha$^{-1}$), indicating weeds could accumulate significant biomass.

Notably, higher biomass measurements, exceeding 10 Mg ha$^{-1}$, were recorded during the year 2020 (as illustrated in Figure 1a). This increase in biomass coincided with sampling dates that accumulated greater GDD (Table 1).

VIs, such as NDVI, are recognized to exhibit reduced sensitivity to changes in leaf area index (LAI) when LAI surpasses a threshold of approximately 3. Beyond this point, the index tends to reach an asymptotic plateau as the soil surface becomes increasingly obscured by leaves (Carlson & Ripley, 1997). In Figure 1, this plateau effect becomes evident at higher biomass levels, coinciding with NDVI values ranging from 0.70 to 0.80. Thieme et al. (2023) also noted saturation within this range, removing biomass values above and NDVI of 0.91. Notably, when examining collected rye biomass exceeding 5 Mg ha$^{-1}$, a trend emerges wherein NDVI values tend to be lower, typically falling within the range of 0.40–0.60 (as depicted in Figure 1b). A similar pattern is observed for NDRE (Figure 1d). This observation suggests that the lower values of NDVI and NDRE may be attributed to reduced ground cover as rye stems elongate (based on GDD) during late growth stages.

Version of Record at: https://doi.org/10.1002/agj2.21554


**TABLE 2** Biomass (Mg ha$^{-1}$) and nitrogen (kg ha$^{-1}$) for control, rye, rye–clover, and rye–vetch plots over the 3 years of the project.

| | Biomass (Mg ha$^{-1}$) | | | Nitrogen (kg ha$^{-1}$) | | | C:N ratio | | |
|---|---|---|---|---|---|---|---|---|---|
| **Cover crop** | **Mean** | **Min.** | **Max.** | **Mean** | **Min.** | **Max.** | **Mean** | **Min.** | **Max.** |
| Control | 1.09 | 0.25 | 4.09 | 22.21 | 2.60 | 158.25 | 21.8 | 10.5 | 38.6 |
| Rye | 4.31 | 0.78 | 16.78 | 61.82 | 14.11 | 245.75 | 31.6 | 13.0 | 67.7 |
| Rye–clover | 6.10 | 1.27 | 21.75 | 124.50 | 27.86 | 414.37 | 20.3 | 12.7 | 36.8 |
| Rye–vetch | 4.93 | 1.28 | 15.54 | 140.84 | 25.13 | 381.85 | 16.5 | 9.0 | 33.9 |

Abbreviation: Max., maximum; Min., minimum.

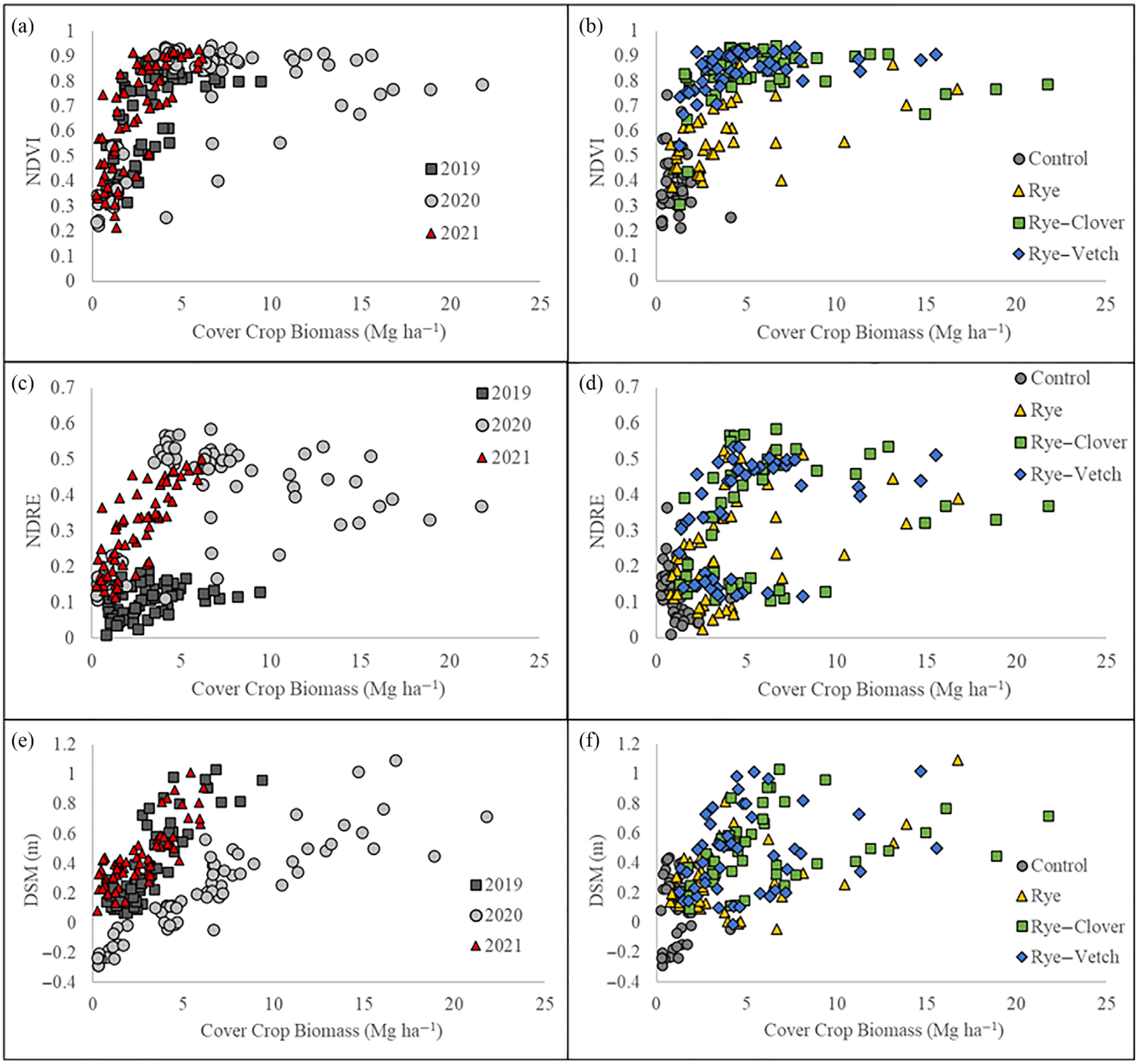


**FIGURE 1** Cover crop biomass (Mg ha$^{-1}$) compared to (a) normalized difference vegetation index (NDVI) by year, (b) NDVI by species, (c) normalized difference red edge index (NDRE) by year, (d) NDRE by species, (e) digital surface mode (DSM) by year, and (f) DSM by species.

Version of Record at: https://doi.org/10.1002/agj2.21554


It is worth highlighting that the inclusion of legumes alongside rye appears to mitigate this effect, resulting in NDVI values reaching a plateau at approximately 0.80, even with comparable biomass levels. Nevertheless, even in the absence of legumes, late-season rye biomass may necessitate distinct modeling or adjustments based on GDD (White et al., 2019; Xia et al., 2021).

For cover crops, red or red-edge saturation has translated into biomass levels between 1.5 and 1.9 Mg ha$^{-1}$ (Jennewein et al., 2022; Prabhakara et al., 2015). These plateaus in VI are based on linear or quadratic plateau analyses of cover crop data, with Jennewein et al. (2022) observing better success with natural log transformations. In this study (Figure 1), we selected the linear plateau model as the best fit for NDVI, NDRE, and the DSM based on AIC. These models exhibited a plateau effect at 3.86, 5.72, and 5.11 Mg ha$^{-1}$, respectively. It is worth noting that the higher biomass plateaus in this study may be attributed to the higher resolution of drone imagery, which ranged from 3.3 to 6.9 cm pixel$^{-1}$, whereas satellite imagery is coarser, ranging from 10 to 30 m satellite resolution. Additionally, our study may benefit from more consistent plot averages through data extraction compared to the studies performed in farmers' fields. Yuan et al. (2019) were able to predict biomass using linear relationships; however, their biomass did not exceed 1.5 Mg ha$^{-1}$.

## 3.2 | Plateau relationships of cover crop nitrogen with NDVI, NDRE, and the DSM

Total N (kg ha$^{-1}$) in cover crops is a product of biomass and %N in the tissue. This relationship means that higher biomass can compensate for lower N concentrations. This principle clarifies why rye–vetch mixtures can exhibit greater total nitrogen content, even when compared to monoculture rye (Table 2), despite having similar biomass levels. As rye progresses through stem elongation, driven by accumulated GDD (Table 1), the C:N ratio tends to increase (Table 2). Conversely, in the case of mixtures containing legumes, which have a higher N content, biomass accumulation is augmented by the presence of N-rich legumes, keeping C:N lower.

For example, in Figure 1b, higher rye biomass did not consistently result in higher NDVI, but those points also had lower N contents (Figure 2b) than similar legume mixtures (Figure 2b). When monoculture rye reaches a biomass level of approximately 16 Mg ha$^{-1}$, the nitrogen content averages around 159 kg N ha$^{-1}$. In contrast, rye + legume mixtures exhibit a wider range, spanning from 285 to 329 kg N ha$^{-1}$, demonstrating the impact of legumes on nitrogen enrichment.

Linear plateaus of N content were 80.9, 139.1, and 75.1 kg N ha$^{-1}$ for NDVI, NDRE, and the DSM, respectively (Figure 2). The NDRE values of cover crop biomass were much lower in 2019, potentially due to differences in the sensors used (Figure 2c).

## 3.3 | Correlations between indices and cover crop characteristics

Correlations between indices with both cover crop biomass and nitrogen were examined across the dataset and by year and species (Table 3). Across the entire dataset (All), the strongest correlation was between NDVI and cover crop N contents (0.63), followed by NDRE and N (0.56). Biomass correlations ranged from 0.49 to 0.53. All of the relationships were positive.

Across species, biomass correlations were variable, with no relationship higher than 0.50 (Table 3). Mixtures of rye + clover only had relationships between biomass and the DSM, while NDRE also correlated with rye + clover N content (Table 3). As anticipated, given the nature of fallow control plots characterized by limited plant growth (Table 2), significant relationships were not observed for most variables, except in the case of biomass and NDRE (Table 3). Notably, the correlation between biomass and NDRE in these control plots was negative, with a coefficient of −0.29.

While it is acknowledged that annual variations in plant growth are influenced by weather and field conditions, examining correlations by year underscores the significance of the DSM. Specifically, the strongest correlations with biomass were observed on an yearly basis, demonstrating a range from $r = 0.79$ to 0.82 for the DSM. However, it is worth noting that the relationship between the DSM and cover crop biomass exhibits variability in slope across different years (Figure 1e), which may affect the DSM's ability to be used over multiple seasons. Some of the variation in the DSM calculations may come from annual ground control point elevations collected by RTK, but the methodology needs further evaluation.

Previous observations in peanut canopy studies have indicated a strong relationship between drone-derived heights and actual measurements, but they were only collected from one season (Sarkar et al., 2020). When mapping larger fields, the use of drone or satellite imagery may not efficiently attain such high resolutions, necessitating lower flying heights and extended flight times (i.e., longer battery life) to achieve comparable results.

## 3.4 | Models to estimate cover crop biomass and nitrogen content

The ability to estimate cover crop biomass and N contents is necessary to evaluate the potential services they provide, including N contributions to cash crops and weed suppression. We used drone-derived indices, the DSM, and GDD

Version of Record at: https://doi.org/10.1002/agj2.21554



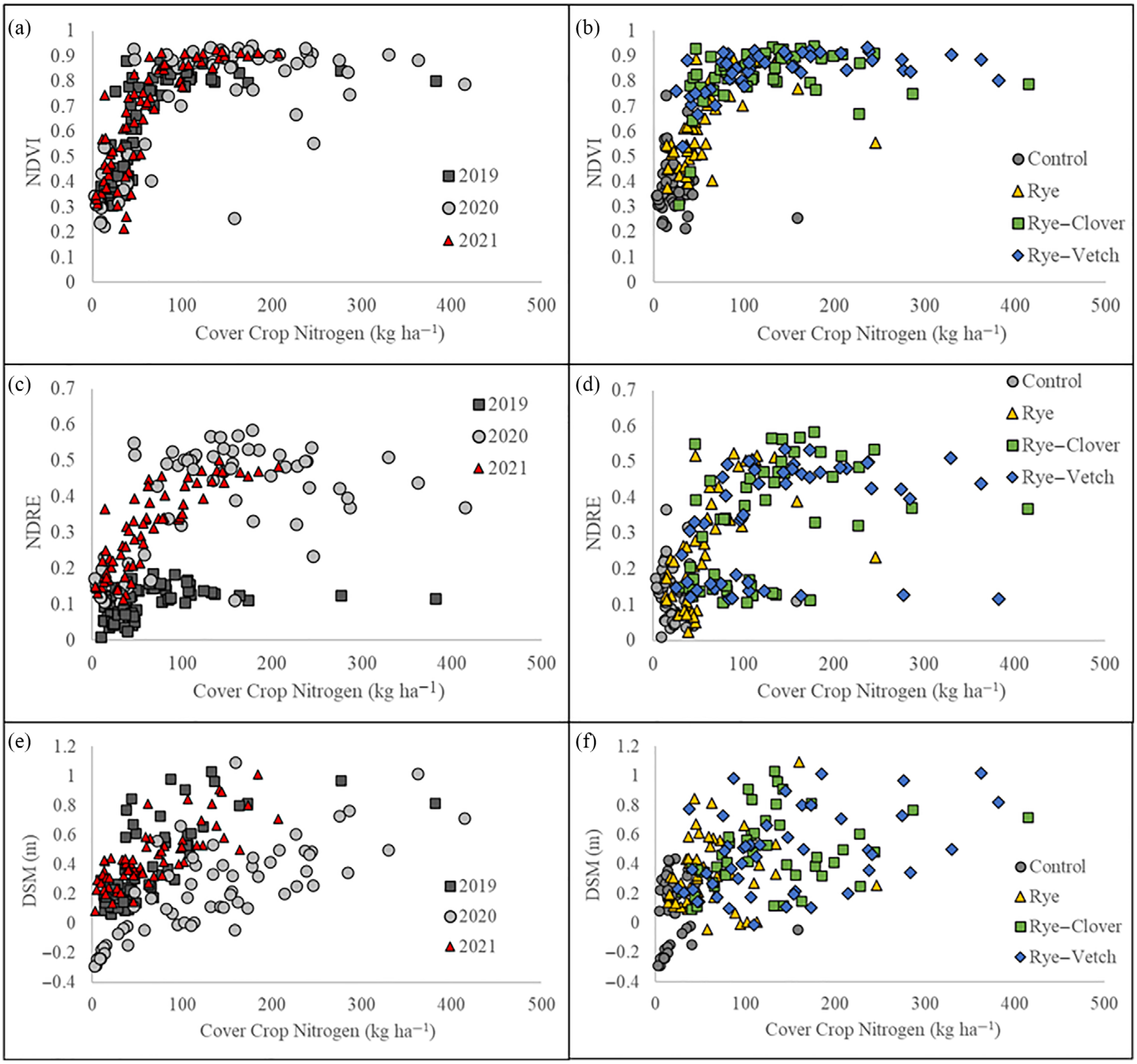


**FIGURE 2** Cover crop nitrogen (kg ha$^{-1}$) compared to (a) normalized difference vegetation index (NDVI) by year, (b) NDVI by species, (c) normalized difference red edge index (NDRE) by year, (d) NDRE by species, (e) digital surface model (DSM) by year, and (f) DSM by species.

to build models of both biomass and N content. For models to estimate the log of cover crop biomass, NDVI was one of the stronger indices (coefficient = 2.81), suggesting that an increase in NDVI predicts larger changes in biomass than NDRE or individual cover crop species (Table 4). Yuan et al. (2019) also observed that drone-derived NDVI was a little better than Green-NDVI or the TVI, but their biomass was less than 1.5 Mg ha$^{-1}$. Individually, GDD could also measure changes in biomass, with a larger role than NDVI, but the DSM was removed by backward selection. The role of species, particularly rye and rye + clover, was significant, but only in interaction with GDD or NDRE, with NDRE showing a negative effect in this context. Vetch had no role in the model, whether individually or as an interaction.

Using satellite-based remote sensing, log-linear models performed better at predicting biomass when using NDRE based on season and species (Jennewein et al., 2022). Spectral indices derived from satellites also performed better for biomass when field measurements (e.g., crop height, ground cover) were included (Xia et al., 2021). In that study, GDD also explained cover crop biomass better than other covariates, similar to its strength in this model. Based on proximal handheld sensors, NDVI has performed better at predicting biomass with earlier dates, prior to saturation, and before freezing events (Prabhakra et al., 2015).

In another drone-based study, a simple red-based ratio (NIR/red) had a linear relationship without log transformation of biomass, while NDVI was curvilinear (Holzhauser et al.,

Version of Record at: https://doi.org/10.1002/agj2.21554


**TABLE 3** Correlations ($r$) between biomass (Mg ha$^{-1}$) and N content (kg N ha$^{-1}$) to drone derived measurements (normalized difference vegetation index [NDVI], normalized difference red edge index [NDRE], and digital surface model [DSM]) and by year (2019, 2020, and 2021).

| | Cover crop biomass (Mg ha$^{-1}$) correlations | | | Cover crop N (kg ha$^{-1}$) correlations | | |
|---|---|---|---|---|---|---|
| | **NDVI** | **NDRE** | **DSM** | **NDVI** | **NDRE** | **DSM** |
| None | NS[†] | −0.29 | NS | NS | NS | NS |
| Rye | 0.50 | 0.46 | 0.43 | 0.57 | 0.58 | NS |
| Rye–clover | NS | NS | 0.38 | NS | 0.41 | 0.34 |
| Rye–vetch | 0.43 | 0.40 | 0.30 | 0.45 | 0.34 | 0.42 |
| 2019 | 0.46 | NS | 0.82 | 0.74 | NS | 0.62 |
| 2020 | −0.28 | −0.46 | 0.79 | NS | NS | 0.58 |
| 2021 | 0.70 | 0.79 | 0.82 | 0.77 | 0.83 | 0.77 |
| All | 0.53 | 0.49 | 0.49 | 0.63 | 0.56 | 0.50 |

*Note*: Differences are significant at $a = 0.05$.
[†]NS, not significant.

**TABLE 4** Models of Log biomass (Mg ha$^{-1}$), log N (kg ha$^{-1}$), and the log C:N based on backward linear regression.

| | Model | Adjusted $R^2$ | RMSE |
|---|---|---|---|
| **Biomass** | Log(Biomass) = −3.71 + (0.009 × GDD) + (2.81 × NDVI) + (0.88 × NDRE) + (0.0003 × GDD × Clover) + (0.0002 × GDD × Rye) − (0.3 × NDRE × Clover) − (0.46 × NDRE × Rye) | 0.75 | 2.16 Mg ha$^{-1}$ |
| | 2.16 Mg ha$^{-1}$ | | |
| **Nitrogen** | Log(Nitrogen) = 0.134 + (0.0008 × GDD) + (1.51 × NDVI) + (1.27 × NDRE) + (0.38 × DSM × Clover) − (0.44 × DSM × Rye) + (0.46 × DSM × Vetch) | 0.76 | 2.28 kg N ha$^{-1}$ |
| **C:N** | Log(C:N) = 2.24 − (0.29 × NDRE) + (0.0003 × GDD × Clover) + (0.0004 × GDD × Rye) + (0.0003 × GDD × Vetch) + (0.06 × DSM × Clover) + (0.18 × DSM × Rye) − (0.49 × DSM × Vetch) | 0.56 | 1.83 |

*Note*: Variables evaluated included growing degree days (GDD), normalized difference vegetation index (NDVI), normalized difference red edge index (NDRE), digital surface model (DSM), and their interactions with cover crop type. The root mean square error (RMSE) values have been back transformed.

2022). For that study, there was a better relationship for red-based indices (e.g., NDVI) for green area index, biomass, and N uptake than red-edge (e.g., NDRE) based indices.

When modeling cover crop N content (log N ha$^{-1}$) in this study, both positive changes in NDVI and NDRE had similar predicting power. The GDD was closer in value to the indices for predicting N content, lower than when estimating biomass. Additionally, the DSM exhibited predictive potential when considering interactions with rye, vetch, and clover. While the log transformation of biomass mitigates the plateau effects observed with NDVI and NDRE, the inclusion of plant height (represented by the DSM) offers promise for accurate total N predictions. Calibration by species and season using exponential models also performed well at predicting N with NDVI ($R^2 = 0.72$–$0.87$), while this study only observed species-level interactions with the DSM (White et al., 2019). Xia et al. (2021), using satellite indices, also found that N contents were best modeled by species, although C:N ratios had a moderate relationship with combined rye and legume N cover crops.

For the C:N ratio in our model, it was observed that NDVI did not significantly contribute to the model's predictive power, as opposed to biomass or N content. Additionally, NDRE exhibited a minor negative relationship with the C:N ratio, with a coefficient of −0.29, matching its ability to respond to chlorophyll and higher N contents. The relationships between the model variables, GDD and the DSM, were found to be dependent on individual cover crop species. Compared to biomass and N contents, GDD had relatively small contributions to the C:N model, and its impact on the ratio varied based on specific cover crop species.

The observed versus predicted values for biomass (Figure 3) have an $R^2$ of 0.77 and a slope of 0.99, which is similar to nitrogen ($R^2 = 0.77$, slope = 0.99) and higher than the C:N ($R^2 = 0.58$, slope = 0.99). This matches the adjusted $R^2$ found in the models (Table 4). While predicting biomass is important for ecosystem services such as weed suppression, predictions of cover crop N may have more interest to both water quality professionals and farmers who desire N credits.

Version of Record at: https://doi.org/10.1002/agj2.21554


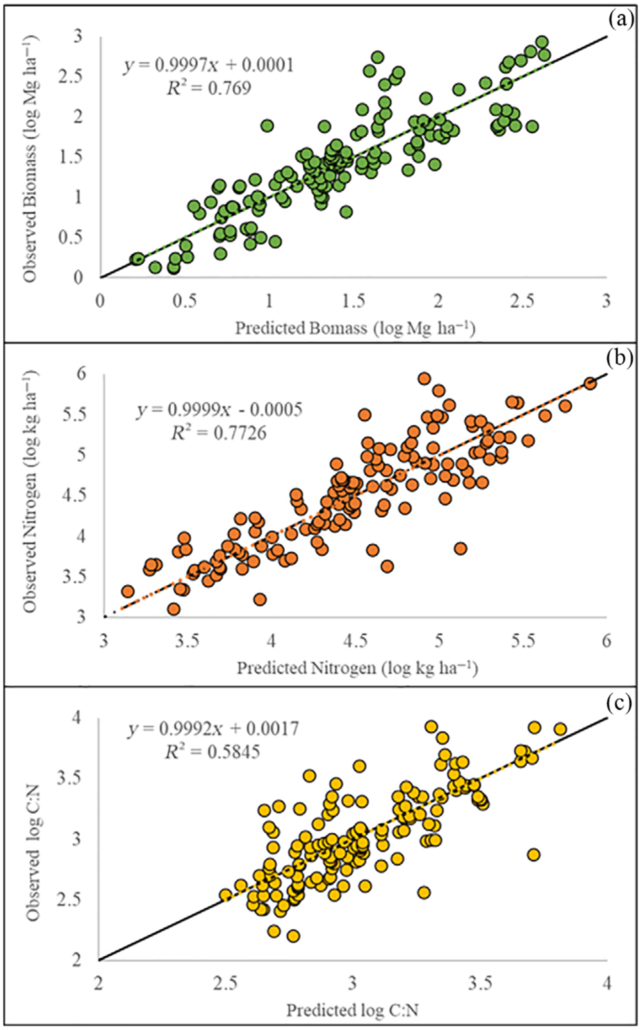


**FIGURE 3** Predicted versus observed relationships for (a) log biomass, (b) log N, and (c) log C:N.

## 4 | CONCLUSIONS

This study focuses on measuring the biomass and N content of rye and rye + legume mixtures using drone imagery. Linear plateau models based on either NDVI, NDRE, or the DSM could predict biomass up to 3.86, 5.72, and 5.11 Mg ha$^{-1}$, respectively. This is higher than the 1.5–1.9 Mg ha$^{-1}$ reported in other remote sensing studies and closer to the standard rye biomass production in the Mid-Atlantic of 5 Mg ha$^{-1}$ (Duiker & Curran, 2005; Jennewein et al., 2022). For N, plateaus for NDVI, NDRE, and the DSM were reached at 80.9, 139.1, and 75.1 kg N ha$^{-1}$, respectively. While the DSM has a strong correlation to biomass, it varied by season and may need its own annual calibration curve. Therefore, improvements in the DSM generation and height estimations should be made to increase the effectiveness of this drone-derived measurement.

Despite the strong correlations between the DSM and biomass, models of log biomass did not select drone-estimated plant heights as a predictor. Instead, NDVI and NDRE were stronger predictors of biomass with a larger contribution from GDD. Based on species, rye and rye + clover were important for predicting biomass when they interacted with GDD or NDRE, but not rye + vetch.

For estimating N contents, GDD, NDVI, and NDRE were individually important. The DSM interacted with the rye and legume mixtures, with the strongest relationship between N and the DSM and rye + vetch combination. For C:N, only NDRE was useful as a single variable, while both GDD and DSM had relationships with each of the cover crop plots.

While drone-derived VIs were successful at estimating higher amounts of biomass than previously measured, relationships for prediction were still complicated by species type. Although the DSM was not useful in predicting biomass, it may prove beneficial in estimating N contents, which is a more important variable to both farmers and water quality experts.

## AUTHOR CONTRIBUTIONS

**Jarrod O. Miller**: Conceptualization; data curation; formal analysis; funding acquisition; investigation; methodology; project administration; software; writing—original draft; writing—review and editing. **Amy L. Shober**: Conceptualization; data curation; formal analysis; funding acquisition; investigation; methodology; project administration; supervision; writing—review and editing. **Jamie Taraila**: Data curation; investigation.

## CONFLICT OF INTEREST STATEMENT

The authors declare no conflicts of interest.

## ORCID

*Jarrod O. Miller* https://orcid.org/0000-0002-5353-233X
*Amy L. Shober* https://orcid.org/0000-0002-5490-6284

## REFERENCES

Balkcom, K. S., Duzy, L. M., Kornecki, T. S., & Price, A. J. (2015). Timing of cover crop termination: Management considerations for the Southeast. *Crop, Forage & Turfgrass Management*, *1*(1), 1–7. https://doi.org/10.2134/cftm2015.0161

Baraibar, B., Murrell, E. G., Bradley, B. A., Barbercheck, M. E., Mortensen, D. A., Kaye, J. P., & White, C. M. (2020). Cover crop mixture expression is influenced by nitrogen availability and growing degree days. *PloS One*, *15*(7), e0235868. https://doi.org/10.1371/journal.pone.0235868

Bean, G. M., Kitchen, N. R., Camberato, J. J., Ferguson, R. B., Fernandez, F. G., Franzen, D. W., Laboski, C. A. M., Nafziger, E. D., Sawyer, J. E., Scharf, P. C., Schepers, J., & Shanahan, J. S. (2018). Active-optical reflectance sensing corn algorithms evaluated over the

United States Midwest corn belt. *Agronomy Journal*, *110*, 2552–2565. https://doi.org/10.2134/agronj2018.03.0217

Boiarskii, B., & Hasegawa, H. (2019). Comparison of NDVI and NDRE indices to detect differences in vegetation and chlorophyll content. *Journal of Mechanics of Continua and Mathematical Sciences*, *4*, 20–29.

Brennan, E. B., & Boyd, N. S. (2012). Winter cover crop seeding rate and variety affects during eight years of organic vegetables: I. Cover crop biomass production. *Agronomy Journal*, *104*(3), 684–698. https://doi.org/10.2134/agronj2011.0330

Butler, T. J., Evers, G. W., Hussey, M. A., & Ringer, L. J. (2002). Rate of leaf appearance in crimson clover. *Crop Science*, *42*(1), 237–241. https://doi.org/10.2135/cropsci2002.2370

Carlson, T. N., & Ripley, D. A. (1997). On the relation between NDVI, fractional vegetation cover, and leaf area index. *Remote Sensing of Environment*, *62*(3), 241–252. https://doi.org/10.1016/S0034-4257(97)00104-1

Corti, M., Cavalli, D., Cabassi, G., Bechini, L., Pricca, N., Paolo, D., Marinoni, L., Vigoni, A., Degano, L., Gallina, P. M., & Marino Gallina, P. (2023). Improved estimation of herbaceous crop aboveground biomass using UAV-derived crop height combined with vegetation indices. *Precision Agriculture*, *24*(2), 587–606. https://doi.org/10.1007/s11119-022-09960-w

Czarnecki, J. M. P., Matese, A., Miles, D. M., Bheemanahalli, R., & Adeli, A. (2023). Evaluating the spectral response of cotton and corn to different cover crops using UAV imagery. In J. V. Stafford (Ed.), *Precision agriculture'23* (pp. 677–683). Wageningen Academic.

Deines, J. M., Guan, K., Lopez, B., Zhou, Q., White, C. S., Wang, S., & Lobell, D. B. (2023). Recent cover crop adoption is associated with small maize and soybean yield losses in the United States. *Global Change Biology*, *29*(3), 794–807. https://doi.org/10.1111/gcb.16489

Dobbs, A. M., Ginn, D., Skovsen, S. K., Yadav, R., Jha, P., Bagavathiannan, M. V., Mirsky, S. B., Reberg-Horton, C. S., & Leon, R. G. (2023). Using structure-from-motion to estimate cover crop biomass and characterize canopy structure. *Field Crops Research*, *302*, 109099. https://doi.org/10.1016/j.fcr.2023.109099

Duiker, S. W., & Curran, W. S. (2005). Rye cover crop management for corn production in the northern Mid-Atlantic region. *Agronomy Journal*, *97*(5), 1413–1418. https://doi.org/10.2134/agronj2004.0317

Finney, D. M., White, C. M., & Kaye, J. P. (2016). Biomass production and carbon/nitrogen ratio influence ecosystem services from cover crop mixtures. *Agronomy Journal*, *108*(1), 39–52. https://doi.org/10.2134/agronj15.0182

Gao, F., & Zhang, X. (2021). Mapping crop phenology in near real-time using satellite remote sensing: Challenges and opportunities. *Journal of Remote Sensing*, *2021*, 8379391.

Garba, I. I., Bell, L. W., & Williams, A. (2022). Cover crop legacy impacts on soil water and nitrogen dynamics, and on subsequent crop yields in drylands: a meta-analysis. *Agronomy for Sustainable Development*, *42*(3), Article 34. https://doi.org/10.1007/s13593-022-00760-0

Holzhauser, K., Räbiger, T., Rose, T., Kage, H., & Kühling, I. (2022). Estimation of biomass and N uptake in different winter cover crops from UAV-based multispectral canopy reflectance data. *Remote Sensing*, *14*(18), 4525. https://doi.org/10.3390/rs14184525

Jennewein, J. S., Lamb, B. T., Hively, W. D., Thieme, A., Thapa, R., Goldsmith, A., & Mirsky, S. B. (2022). Integration of satellite-based optical and synthetic aperture radar imagery to estimate winter cover crop performance in cereal grasses. *Remote Sensing*, *14*(9), 2077. https://doi.org/10.3390/rs14092077

Kümmerer, R., Noack, P. O., & Bauer, B. (2023). Using high-resolution UAV imaging to measure canopy height of diverse cover crops and predict biomass. *Remote Sensing*, *15*(6), 1520. https://doi.org/10.3390/rs15061520

Maresma, A., Chamberlain, L., Tagarakis, A., Kharel, T., Godwin, G., Czymmek, K. J., Shields, E., & Ketterings, Q. M. (2020). Accuracy of NDVI-derived corn yield predictions is impacted by time of sensing. *Computers and Electronics in Agriculture*, *169*, 105236. https://doi.org/10.1016/j.compag.2020.105236

Otte, B., Mirsky, S., Schomberg, H., Davis, B., & Tully, K. (2019). Effect of cover crop termination timing on pools and fluxes of inorganic nitrogen in no-till corn. *Agronomy Journal*, *111*(6), 2832–2842. https://doi.org/10.2134/agronj2018.10.0699

Poley, G. L., & McDermid, G. J. (2020). A systematic review of the factors influencing the estimation of vegetation aboveground biomass using unmanned aerial systems. *Remote Sensing*, *12*(7), 1052. https://doi.org/10.3390/rs12071052

Poffenbarger, H. J., Mirsky, S. B., Weil, R. R., Maul, J. E., Kramer, M., Spargo, J. T., & Cavigelli, M. A. (2015). Biomass and nitrogen content of hairy vetch–cereal rye cover crop mixtures as influenced by species proportions. *Agronomy Journal*, *107*(6), 2069–2082. https://doi.org/10.2134/agronj14.0462

Prabhakara, K., Hively, W. D., & McCarty, G. W. (2015). Evaluating the relationship between biomass, percent groundcover and remote sensing indices across six winter cover crop fields in Maryland, United States. *International Journal of Applied Earth Observation and Geoinformation*, *39*, 88–102. https://doi.org/10.1016/j.jag.2015.03.002

Pantoja, J. L., Woli, K. P., Sawyer, J. E., & Barker, D. W. (2016). Winter rye cover crop biomass production, degradation, and nitrogen recycling. *Agronomy Journal*, *108*(2), 841–853. https://doi.org/10.2134/agronj2015.0336

Reed, H. K., Karsten, H. D., Curran, W. S., Tooker, J. F., & Duiker, S. W. (2019). Planting green effects on corn and soybean production. *Agronomy Journal*, *111*(5), 2314–2325. https://doi.org/10.2134/agronj2018.11.0711

Sangjan, W., McGee, R. J., & Sankaran, S. (2022). Optimization of UAV-based imaging and image processing orthomosaic and point cloud approaches for estimating biomass in a forage crop. *Remote Sensing*, *14*(10), 2396. https://doi.org/10.3390/rs14102396

Sarkar, S., Cazenave, A.-B., Oakes, J., McCall, D., Thomason, W., Abbot, L., & Balota, M. (2020). High-throughput measurement of peanut canopy height using digital surface models. *The Plant Phenome Journal*, *3*, e20003. https://doi.org/10.1002/ppj2.20003

Thieme, A., Hively, W. D., Gao, F., Jennewein, J., Mirsky, S., Soroka, A., Keppler, J., Bradley, D., Skakun, S., & McCarty, G. W. (2023). Remote sensing evaluation of winter cover crop springtime performance and the impact of delayed termination. *Agronomy Journal*, *115*(1), 442–458. https://doi.org/10.1002/agj2.21207

Teasdale, J. R., Mirsky, S. B., Spargo, J. T., Cavigelli, M. A., & Maul, J. E. (2012). Reduced-tillage organic corn production in a hairy vetch cover crop. *Agronomy Journal*, *104*(3), 621–628. https://doi.org/10.2134/agronj2011.0317

White, C. M., Bradley, B., Finney, D. M., & Kaye, J. P. (2019). Predicting cover crop nitrogen content with a handheld normalized difference vegetation index meter. *Agricultural & Environmental Letters*, *4*(1), 190031. https://doi.org/10.2134/ael2019.08.0031

Xia, Y., Guan, K., Copenhaver, K., & Wander, M. (2021). Estimating cover crop biomass nitrogen credits with Sentinel-2 imagery and site covariates. *Agronomy Journal*, *113*, 1084–1101. https://doi.org/10.1002/agj2.20525

Yuan, M., Burjel, J. C., Isermann, J., Goeser, N. J., & Pittelkow, C. M. (2019). Unmanned aerial vehicle–based assessment of cover crop biomass and nitrogen uptake variability. *Journal of Soil and Water Conservation*, *74*(4), 350–359. https://doi.org/10.2489/jswc.74.4.350

**How to cite this article:** Miller, J. O., Shober, A. L., & Taraila, J. (2024). Assessing relationships of cover crop biomass and nitrogen content to multispectral imagery. *Agronomy Journal*, 1–11. https://doi.org/10.1002/agj2.21554